Original Article | Cardiovascular Imaging

eISSN 2005-8330
https://doi.org/10.3348/kjr.2020.1291
Korean J Radiol 2021;22(10):1619-1627

Korean Journal of Radiology
KJR

Left Ventricular Remodeling in Patients with Primary Aldosteronism: A Prospective Cardiac Magnetic Resonance Imaging Study

Tao Wu[1], Yan Ren[2], Wei Wang[2], Wei Cheng[1], Fangli Zhou[2], Shuai He[1], Xiumin Liu[1], Lei Li[1], Lu Tang[1], Qiao Deng[1, 3], Xiaoyue Zhou[4], Yucheng Chen[5], Jiayu Sun[1]

Departments of [1]Radiology, [2]Endocrinology and Metabolism, and [5]Cardiology, West China Hospital, Sichuan University, Chengdu, China; [3]North Sichuan Medical College, Nanchong, China; [4]MR Collaboration, Siemens Healthcare, Shanghai, China

Objective: This study used cardiac magnetic resonance imaging (MRI) to compare the characteristics of left ventricular remodeling in patients with primary aldosteronism (PA) with those of patients with essential hypertension (EH) and healthy controls (HCs).

Materials and Methods: This prospective study enrolled 35 patients with PA, in addition to 35 age- and sex-matched patients with EH, and 35 age- and sex-matched HCs, all of whom underwent comprehensive clinical and cardiac MRI examinations. The analysis of variance was used to detect the differences in the characteristics of left ventricular remodeling among the three groups. Univariable and multivariable linear regression analyses were used to determine the relationships between left ventricular remodeling and the physiological variables.

Results: The left ventricular end-diastolic volume index (EDVi) (mean ± standard deviation [SD]: 85.1 ± 13.0 mL/m^2 for PA, 75.9 ± 14.3 mL/m^2 for EH, and 77.3 ± 12.8 mL/m^2 for HC; p = 0.010), left ventricular end-systolic volume index (ESVi) (mean ± SD: 35.2 ± 9.8 mL/m^2 for PA, 30.7 ± 8.1 mL/m^2 for EH, and 29.5 ± 7.0 mL/m^2 for HC; p = 0.013), left ventricular mass index (mean ± SD: 65.8 ± 16.5 g/m^2 for PA, 56.9 ± 12.1 g/m^2 for EH, and 44.1 ± 8.9 g/m^2 for HC; p < 0.001), and native T1 (mean ± SD: 1224 ± 39 ms for PA, 1201 ± 47 ms for EH, and 1200 ± 44 ms for HC; p = 0.041) values were higher in the PA group compared to the EH and HC groups. Multivariable linear regression demonstrated that log (plasma aldosterone-to-renin ratio) was independently correlated with EDVi and ESVi. Plasma aldosterone was independently correlated with native T1.

Conclusion: Patients with PA showed a greater degree of ventricular hypertrophy and enlargement, as well as myocardial fibrosis, compared to those with EH. Cardiac MRI T1 mapping can detect left ventricular myocardial fibrosis in patients with PA.

Keywords: *Hyperaldosteronism; Essential hypertension; Magnetic resonance imaging; Ventricular remodeling*

INTRODUCTION

Primary aldosteronism (PA) is a major form of secondary hypertension, which is caused by excessive aldosterone secretion from the adrenal glands [1]. The proportion of PA in the hypertensive population remains unclear. Some studies reported that patients with PA accounted for > 5%, and possibly > 10%, of patients with hypertension [2]. Patients with PA are at a higher risk of experiencing cardiovascular events, including coronary artery disease,

Received: November 2, 2020 **Revised:** April 7, 2021 **Accepted:** April 25, 2021
This work was supported by grants from the Key R & D projects in Sichuan Province (No. 2020YFS0123) and 1·3·5 Project for Disciplines of Excellence-Clinical Research Incubation Project (2018HXFH009).
Corresponding author: Jiayu Sun, MD, Department of Radiology, West China Hospital, Sichuan University, Guoxue Xiang No. 37, Chengdu, Sichuan 610041, China.
• E-mail: cardiac_wchscu@163.com

atrial fibrillation, and heart failure compared to patients with essential hypertension (EH) [3,4]. Ventricular remodeling plays an essential role in the pathogenesis, progression, and prognosis of heart disease [5,6]. Therefore, we explored ventricular remodeling in patients with early-stage PA in comparison with patients with EH and healthy controls (HCs). A better understanding of ventricular remodeling may guide the prompt implementation of interventions after the diagnosis of PA and prevent ventricular remodeling.

Echocardiography is the imaging modality of choice for assessing ventricular remodeling due to its low cost and convenience of operation [5,7]. Several echocardiographic studies have demonstrated that diastolic dysfunction was significantly higher in patients with PA compared to those with EH [8-10]. However, echocardiography is beset by limitations, such as its relatively low signal-to-noise ratio, repeatability, and acoustic window [11,12], which tend to become more pronounced during imaging of the early stages of ventricular remodeling.

Cardiac magnetic resonance imaging (MRI), a steady and precise imaging modality, is widely used to assess ventricular function and dimensions, while late-gadolinium enhancement (LGE) can also be used to evaluate focal myocardial fibrosis. However, LGE depends on the visual comparison between damaged and undamaged myocardium; thus, it cannot detect diffuse myocardial fibrosis [13-15]. T1 mapping derived from cardiac MRI has emerged as a sensitive method that can detect early changes in the characteristics of myocardial tissue, especially quantitative changes in diffuse myocardial fibrosis that exist during the early stages of ventricular remodeling [16-21]. However, few studies have comprehensively investigated the function of T1 mapping with cardiac MRI for examining ventricular function and tissue characteristics to distinguish between patients with EH and those with PA. In a recent study, Redheuil et al. [22] found that patients with PA had a significantly larger left ventricular (LV) chamber, greater LV mass, and greater extracellular volume (ECV) compared to patients with EH. Nevertheless, the sample size of their study was small, which necessitated the validation of their results; moreover, the influence of ethnicity on LV remodeling cannot be ignored [23]. Therefore, the present study aimed to determine the LV remodeling characteristics of patients with PA using cardiac MRI by comparing the LV structure, function, and tissue characteristics among patients with PA, patients with EH, and HCs.

MATERIALS AND METHODS

Each study participant provided written informed consent for enrollment in this prospective study, which was approved by the Local Ethics Committee in accordance with the Declaration of Helsinki, as revised in 2013 (IRB No. 2016 355). Patients with PA, and age- and sex-matched adult patients with EH, and HCs were recruited between September 2018 and May 2019. The diagnosis of PA was based on the 2016 guidelines [2]. Participants were matched for age within 5 years and sex-matched at a proportion of 1:1:1. Participants with a plasma aldosteroneto-renin ratio (ARR) ≥ 30, those with an ARR ≥ 20, and plasma renin activity (PRA) < 1 ng/mL/h, and participants with a plasma aldosterone concentration ≥ 15 ng/dL were further evaluated using confirmatory tests. Confirmatory tests included a saline infusion and/or a captopril challenge. A post-infusion plasma aldosterone concentration of > 10 ng/dL was the cut-off value for PA with the saline infusion test, while a 30% captopril-induced suppression of plasma aldosterone after the captopril challenge was indicative of PA. The diagnostic criterion for patients with EH was a systolic blood pressure (SBP) ≥ 140 mm Hg or diastolic blood pressure (DBP) ≥ 90 mm Hg to eliminate the possibility of secondary hypertension. HCs were included if they did not have any known chronic disease (including cardiovascular disease, neurological disease, chronic lung disease, diabetes mellitus, cancer, autoimmune disease, etc.), or systemic infection, severe trauma, or history of surgery within the past month. This information was obtained through medical history questionnaires. All HCs underwent a physical examination to exclude the possibility of abnormal physical signs. HCs were also excluded if they demonstrated abnormal cardiac structure, function, or tissue characteristics on cardiac MRI.

Participants were excluded if they met the following criteria: 1) patients with known cardiovascular disease, such as myocardial infarction, unstable angina, atrial fibrillation, severe arrhythmia, systolic heart failure, cardiomyopathy, or valvular disease with the exception of hypertension; 2) patients with cardioverter defibrillator or pacemaker implantation; 3) patients with claustrophobia or other conditions that could lead to scan termination; and 4) participants with artifacts on MRI. The baseline characteristics, including the demographic data, laboratory examination results, and cardiac MRI-derived parameters, were collected.

https://doi.org/10.3348/kjr.2020.1291

Korean Journal of Radiology
KJR

Cardiac MRI Acquisition

All participants underwent cardiac MRI using a 3T scanner (MAGNETOM Trio A Tim System; Siemens Healthcare) with an 18-channel phased-array body coil combined with a spine coil. Image acquisition was performed as per the standard protocol [24]. Ventricular function was assessed using balanced steady-state free precession cine images in short-axis planes from the base of the heart to the apex. The parameters were as follows: repetition time (TR), 3.4 ms; echo time (TE), 1.3 ms; voxel size, 1.4 x 1.3 x 8 mm^3; flip angle (FA), 50°; field of view (FOV), 320–340 mm^2; matrix size, 256 x 144; and cardiac time frame temporal resolution, 42 ms. The native T1 value was assessed using a motion-corrected modified Look-Locker inversion recovery sequence (MOLLI) with a scan scheme of 5b(3b)3b (where b stands for heartbeat) on the mid-ventricular short-axis slice. The imaging parameters for MOLLI were as follows: total acquisition, 11 heartbeats; TR, 2.9 ms; TE, 1.12 ms; in-plane spatial resolution, 2.4 x 1.8 mm; FA, 35°; bandwidth, 930 Hz/pixel; inversion time (TI) of the first experiment, 100 ms; TI increment, 80 ms; parallel imaging, 2; and matrix, 192 x 144. LGE images were acquired 10–15 minutes after injection of the gadolinium contrast agent (0.15 mmoL/kg) using the inversion recovery method with phase-sensitive reconstruction (PSIR) on identical views as the cine images in the short- and long-axis planes (TR, 700 ms; TE, 1.56 ms; FA, 20°; and matrix, 256 x 244). T1 measurements were repeated in the same mid-ventricular slice approximately 15 minutes post-injection using the same MOLLI sequence (scan scheme: 4b(1b)3b(1b)2b). Hematocrit (HCT) was assessed within 24 hours of cardiac MRI to calculate the ECV. The short-axial cine and T1 mapping imaging are demonstrated in Figure 1.

Cardiac MRI Analysis

Anonymized cardiac MRI data were analyzed by two blinded independent observers (each with experience of more than 3 years and 800 cases) using dedicated software (Argus; Siemens Healthcare). The LV and right ventricular (RV) volumetric parameters, including the LV end-diastolic volume index (EDVi), LV end-systolic volume index (ESVi), LV ejection fraction (EF), RV-EDVi, RV-ESVi, RVEF, and LV mass index (Massi) were obtained from the short-axis cine images.

LGE Assessment

The presence of myocardial LGE was determined by consensual agreement of two blinded independent observers

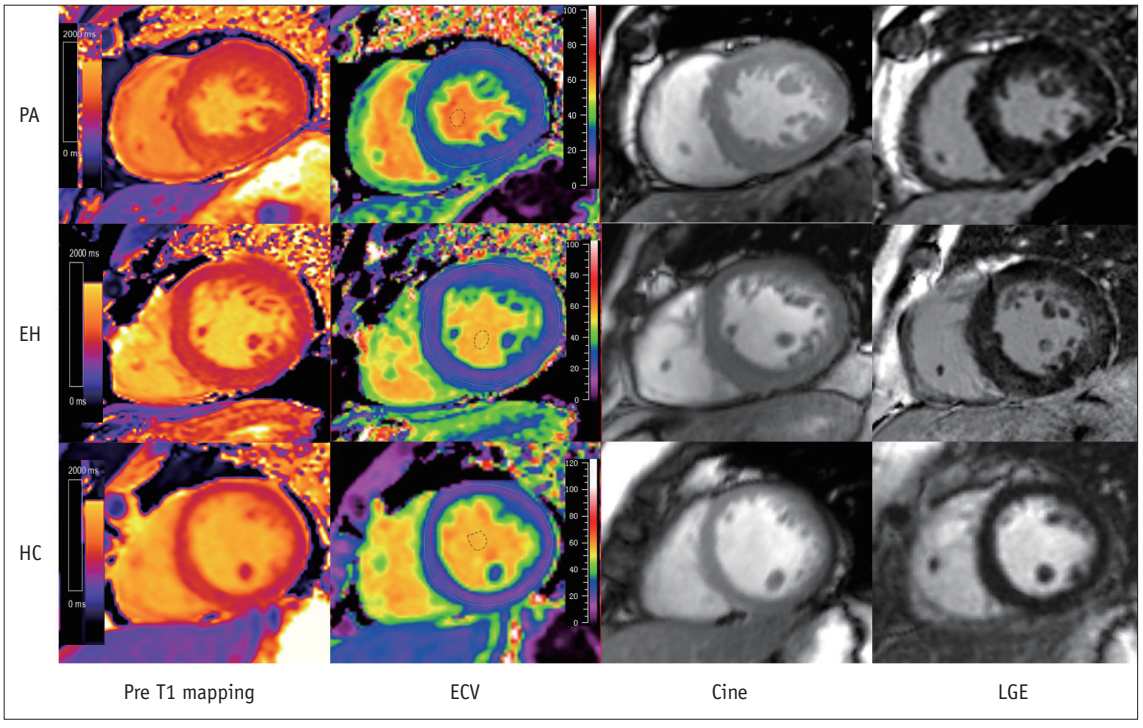

Fig. 1. Comparison of native T1, ECV, cine, and LGE images among patients with PA, patients with EH, and HCs. T1 mapping; PA: 1296 ms, EH: 1193 ms, HC: 1167 ms. ECV; PA: 27.1%, EH: 24.1%, HC: 23.1%. ECV = extracellular volume, EH = essential hypertension, HC = healthy control, LGE = late gadolinium enhancement, PA = primary aldosteronism

https://doi.org/10.3348/kjr.2020.1291

who reviewed all the PSIR images. LGE was determined to be present if local myocardial enhancement was visible on the short-axis and corresponding long-axis views.

T1 Mapping Assessment

The endocardial and epicardial contours were traced manually on the pre- and post-contrast T1 mapping images on the mid-ventricular LV short-axis slice for global analysis. A myocardial region of interest was carefully demarcated, excluding the papillary muscles, trabeculae, blood pool, and epicardial tissue. The mean myocardial native T1 values were acquired using post-processing software (Qmass 7.6; Medis) based on the MOLLI images. Meanwhile, a region of interest was created in the blood pool of the LV cavity on the pre- and post-contrast T1-mapping images to acquire the blood T1 (Supplementary Fig. 1). The ECV was calculated from the combined T1 and HCT values using the following equation [25]:

$$ECV = (1 - HCT)\, x\, \frac{\left[\frac{1}{T1_{myocardial\ post-contrast}} - \frac{1}{T1_{myocardial\ pre-contrast}}\right]}{\left[\frac{1}{T1_{blood\ post-contrast}} - \frac{1}{T1_{blood\ pre-contrast}}\right]}$$

Statistical Analysis

The Kolmogorov-Smirnov test was employed to determine the normality of distribution of the continuous variables. Normally distributed continuous variables were expressed as the mean ± standard deviation, while continuous variables with non-normal distribution were expressed as the median and interquartile range. Differences in the continuous variables among the three groups were analyzed using the analysis of variance. Multiple post-hoc comparisons were performed using Fisher's least significant difference when a significant inter-group difference was detected. Comparisons involving only two groups were conducted using Student's *t* test or the Mann-Whitney U test for continuous variables and the chi-squared test for categorical variables. Univariable and multivariable linear regression were used to analyze the relationships between the LV remodeling parameters and physiological variables. PRA and ARR were log-transformed for the regression analysis, owing to their non-normal distribution. Variables with a p value of < 0.10 on univariable regression were included in the multivariable regression analysis. Standardized β and adjusted R^2 values were calculated. Statistical analysis was performed using IBM SPSS Statistics for Windows, Version 19.0. (IBM Corp.). p values < 0.05 were considered statistically significant.

RESULTS

Clinical Characteristics

A total of 105 participants were included in this prospective study: 35 patients with PA, 35 age- and sex-matched patients with EH, and 35 age- and sex-matched HCs. The participants' clinical characteristics are summarized in Table 1. The HCs had the lowest body mass index (PA: 25.6 ± 3.4 kg/m^2, EH: 25.4 ± 2.9 kg/m^2, HC: 22.3 ± 3.3 kg/m^2;

Table 1. Demographic and Clinical Characteristics of Patients with PA, Patients with EH, and HCs

Characteristic	PA (n = 35)	EH (n = 35)	HC (n = 35)	*P*
Sex, male:female	14:21	14:21	14:21	NA
Age, years	44 ± 11	43 ± 11	44 ± 14	0.968
BMI, kg/m^2	25.6 ± 3.4	25.4 ± 2.9	22.3 ± 3.3	< 0.001
Heart rate, min^{-1}	81 ± 13	85 ± 12	76 ± 8	0.002
SBP, mm Hg	146 ± 16	144 ± 13	121 ± 10	< 0.001
DBP, mm Hg	95 ± 13	96 ± 11	73 ± 7	< 0.001
HCT, %	41 ± 4	42 ± 4	43 ± 3	0.042
Ald, ng/dL	37.6 ± 17.7	28.8 ± 8.9	NA	0.011*
ARR, ng/dL per ng/mL/h	108.6 (64.1–617.0)	7.8 (4.1–12.0)	NA	< 0.001*
PRA, ng/mL/h	0.23 (0.07–0.46)	4.23 (2.28–7.14)	NA	< 0.001*
Serum potassium, mmoL/L	3.5 ± 0.5	3.9 ± 0.4	NA	0.003*
Hypertension course, months	36 (8–72)	24 (5–2)	NA	0.580*

Data are mean ± standard deviation, except for ARR, PRA, and hypertension course presented as median (interquartile range) and sex presented as patient number. *p* values are for comparing the three groups using analysis of variance, except for characteristics asterisked (*) for which the groups were compared using the student's *t* test or the Mann–Whitney U test. Ald = aldosterone, ARR = plasma aldosterone-to-renin ratio, BMI = body mass index, DBP = diastolic blood pressure, ECV = extracellular volume, EH = essential hypertension, HC = healthy control, HCT = hematocrit, NA = not applicable, PA = primary aldosteronism, PRA = plasma renin activity, SBP = systolic blood pressure

https://doi.org/10.3348/kjr.2020.1291

Korean Journal of Radiology
KJR

$p < 0.001$), SBP (PA: 146 ± 16 mm Hg, EH: 144 ± 13 mm Hg, HC: 121 ± 10 mm Hg; $p < 0.001$), DBP (PA: 95 ± 13 mm Hg, EH: 96 ± 11 mm Hg, HC: 73 ± 7 mm Hg; $p < 0.001$), and heart rate (PA: 81 ± 13 min^{-1}, EH: 85 ± 12 min^{-1}, HC: 76 ± 8 min^{-1}; $p = 0.002$) of all three groups, as well as the highest HCT percentage (PA: 41% ± 4%, EH: 42% ± 4%, HC: 43% ± 3%; $p = 0.042$).

Comparison of Cardiac MRI Parameters

The LV volume, systolic function, and mass index of the three groups are displayed in Table 2. The EDVi (PA: 85.1 ± 13.0 mL/m^2, EH: 75.9 ± 14.3 mL/m^2, HC: 77.3 ± 12.8 mL/m^2; $p = 0.01$), ESVi (PA: 35.2 ± 9.8 mL/m^2, EH: 30.7 ± 8.1 mL/m^2, HC: 29.5 ± 7.0 mL/m^2; $p = 0.013$), and Massi (PA: 65.8 ± 16.5 g/m^2, EH: 56.9 ± 12.1 g/m^2, HC: 44.1 ± 8.9 g/m^2; $p < 0.001$) were the highest in the PA group. However, statistically significant differences were not observed in the LVEF, RV-EDVi, RV-ESVi, or RVEF among the three groups.

Comparison of Cardiac MRI Tissue Characteristics

LGE was observed in 2 patients (5.7%) with PA. Enhancement was observed at the inferior insertion point in one patient, while patchy enhancement was observed over the anterior lateral wall in the other. LGE also presented as patchy enhancement over the inferior lateral wall in 1 patient (2.8%) with EH. However, no significant difference was observed in the LGE in the PA and EH groups. The native T1 and ECV values are presented in Table 2. Patients with PA had a significantly higher native T1 values compared to patients with EH and the HCs (PA: 1224 ± 39 ms, EH: 1201 ± 47 ms, HC: 1200 ± 44 ms; $p = 0.041$), while the ECV was similar among the three groups.

Analysis of Factors Related to Ventricular Remodeling

Linear regression analysis was performed to determine the factors influencing the LV remodeling parameters, including the EDVi, ESVi, Massi, and native T1 (Tables 3, 4).

Table 2. Comparison of Cardiac Magnetic Resonance Parameters among Patients with PA, Patients with EH, and HCs

	PA (n = 35)	EH (n = 35)	HC (n = 35)	*P* (ANOVA)	*P* (Post-Hoc Test)		
					PA vs. EH	PA vs. HC	EH vs. HC
EDVi, mL/m^2	85.1 ± 13.0	75.9 ± 14.3	77.3 ± 12.8	0.010	0.005	0.015	0.681
ESVi, mL/m^2	35.2 ± 9.8	30.7 ± 8.1	29.5 ± 7.0	0.013	0.027	0.005	0.529
LVEF, %	59.0 ± 7.3	59.7 ± 5.7	62.1 ± 4.4	0.081	NA	NA	NA
Massi, g/m^2	65.8 ± 16.5	56.9 ± 12.1	44.1 ± 8.9	< 0.001	0.005	< 0.001	< 0.001
RV-EDVi, mL/m^2	74.1 ± 13.5	68.7 ± 13.2	68.2 ± 15.4	0.154	NA	NA	NA
RV-ESVi, mL/m^2	34.7 ± 9.8	31.4 ± 7.8	33.4 ± 10.5	0.340	NA	NA	NA
RVEF, %	53.5 ± 8.8	54.5 ± 5.7	52.8 ± 7.7	0.619	NA	NA	NA
Native T1, ms	1224 ± 39	1201 ± 47	1200 ± 44	0.041	0.031	0.027	0.954
ECV, %	26.2 ± 2.8	25.1 ± 3.4	25.8 ± 2.6	0.286	NA	NA	NA

All data are presented as mean ± standard deviation. ANOVA = analysis of variance, ECV = extracellular volume, EDVi = end-diastolic volume index, EF = ejection fraction, EH = essential hypertension, ESVi = left ventricular end-systolic volume index, HC = healthy control, LV = left ventricular, Massi = left ventricular mass index, NA = not applicable, PA = primary aldosteronism, RV = right ventricular

Table 3. Univariable and Multivariable Linear Regression Analysis of EDVi and ESVi in Patients with PA (n = 35)

	EDVi ($R^2 = 0.364$)				ESVi ($R^2 = 0.102$)			
	Univariable		Multivariable		Univariable		Multivariable	
	β	*P*	β	*P*	β	*P*	β	*P*
Age, years	0.141	0.419			0.182	0.296		
Sex	0.180	0.301			0.089	0.611		
BMI, kg/m^2	-0.061	0.728			0.009	0.959		
SBP, mm Hg	0.435	0.009	0.303	0.041	0.120	0.494		
DBP, mm Hg	0.281	0.102			0.028	0.874		
Ald, ng/dL	0.212	0.222			0.187	0.282		
logARR	0.458	0.006	0.338	0.024	0.359	0.034	0.359	0.034
Serum potassium, mmol/L	-0.197	0.258			-0.190	0.274		
Hypertension course, months	0.410	0.014	0.326	0.025	0.348	0.041	0.307	0.060

Ald = aldosterone, ARR = plasma aldosterone-to-renin ratio, BMI = body mass index, DBP = diastolic blood pressure, EDVi = left ventricular end-diastolic volume index, ESVi = left ventricular end-systolic volume index, PA = primary aldosteronism, SBP = systolic blood pressure

https://doi.org/10.3348/kjr.2020.1291

Table 4. Univariable and Multivariable Linear Regression Analysis of Native T1 and Massi in Patients with PA (n = 35)

	Native T1 (R^2 = 0.350)				Massi (R^2 = 0.376)			
	Univariable		Multivariable		Univariable		Multivariable	
	β	*P*	β	*P*	β	*P*	β	*P*
Age, years	0.076	0.666			0.017	0.925		
Sex	-0.536	0.001	-0.549	< 0.001	0.445	0.007	0.408	0.005
BMI, kg/m^2	-0.100	0.568			-0.194	0.265		
SBP, mm Hg	0.032	0.853			0.497	0.002	0.465	0.002
DBP, mm Hg	0.055	0.752			0.217	0.210		
Ald, ng/dL	0.295	0.085	0.318	0.028	0.110	0.530		
logARR	0.204	0.241			0.134	0.441		
Serum potassium, mmoL/L	0.068	0.696			-0.365	0.031	-0.087	0.578
Hypertension course, months	-0.010	0.956			0.356	0.036	0.217	0.123

Ald = aldosterone, ARR = plasma aldosteroneto-renin ratio, BMI = body mass index, DBP = diastolic blood pressure, Massi = left ventricular mass index, PA = primary aldosteronism, SBP = systolic blood pressure

We found that logARR was independently associated with EDVi (β = 0.338, *p* = 0.024) and ESVi (β = 0.359, *p* = 0.034), respectively, and that plasma aldosterone levels were independently associated with native T1 (β = 0.318, *p* = 0.028).

DISCUSSION

In this study, we used cardiac MRI to analyze the structure, function, and tissue characteristics of the LV in 35 patients with PA and compared them with the corresponding parameters in 35 patients with EH and 35 HCs. Our results demonstrated that patients with PA had myocardial hypertrophy and ventricular enlargement with significantly higher Massi, EDVi, and ESVi values compared to patients with EH and the HCs. Patients with PA also demonstrated a reduction in the LVEF. The native T1 value was higher in patients with PA; however, no significant difference was observed in the ECV of patients with PA, patients with EH, and HCs. The EDVi, ESVi, and native T1 were associated with logARR.

In our study, the EDVi and ESVi values were higher in patients with PA compared to those with EH. These results are inconsistent with previous studies, which reported that the LV geometry was similar in patients with PA and those with EH [8,26,27]. However, Gaddam et al. [28] found that only the EDVi was higher in patients with PA compared to those with EH. Most previous studies used echocardiography to measure cardiac volume. Furthermore, Freel et al. [27] study used cardiac MRI to measure cardiac volume, but their patients were older and primarily men, and did not include a multivariable regression analysis of age and sex. Herein, we found that patients with PA demonstrated a reduction in the LVEF compared to the HCs, and these results were contrary to those of Mark et al. [29]. However, Mark et al. [29] did not match patients with PA, patients with EH, and the HCs by age and sex, which could have influenced the LVEF. Although Su et al. [30] found no difference between patients with PA and HCs, the two groups were only matched for age.

Several previous studies reported no difference in the Massi between patients with PA and patients with EH [8,27,28]; however, our results demonstrated a greater Massi in the PA group compared to the EH group. Nevertheless, our findings are supported by animal studies, which demonstrated that a chronic elevation in aldosterone can cause LV hypertrophy [31-33]. Moreover, the course of hypertension was significantly shorter in the patients in our study course compared to other studies, which may explain the inconsistency in the results. Heterogeneity in the course of hypertension and sex distribution may also explain these discrepancies. This implies that aldosterone can directly stimulate hypertrophy of the ventricular cardiomyocytes in the early stages of hypertension in PA.

The PA group in our study had a higher native T1 value, suggesting that patients with PA have more severe myocardial fibrosis; however, the ECV was similar in the PA and EH groups, refuting this theory. Our ECV results are consistent with those of Grytaas et al. [34], who did not detect myocardial fibrosis in patients with PA, when compared to HCs. The native T1 values and ECV parameters are associated with diffuse myocardial fibrosis [35-38]. One study indicated that the native T1 possessed a higher discriminatory performance than that of the ECV [38]. In

https://doi.org/10.3348/kjr.2020.1291

Korean Journal of Radiology
KJR

this study, patients with PA and EH had a relatively shorter course of hypertension, and all patients with PA had been diagnosed recently, implying that the alterations in the myocardium of patients with PA may include myocardial fibrosis, in contrast to patients in the early stages of hypertension (early EH). In our study, patients with PA demonstrated more severe ventricular remodeling compared to patients with EH. This cannot be explained solely by the greater degree of hypertension, since the baseline blood pressure was balanced between the two groups. Instead, we found that the ARR and plasma aldosterone were independently correlated with LV remodeling parameters in patients with PA. Hence, we speculated that the high levels of plasma aldosterone contributed to myocardial damage in patients with PA. In a recent study, Redheuil et al. [22] also found that patients with PA had a significantly larger LV chamber and greater LV mass compared to patients with EH. However, they found that the ECV was significantly greater in patients with PA compared to patients with EH, while the native T1 did not differ significantly between the two groups. It is worth noting that the baseline plasma aldosterone levels were significantly lower in our study compared to their study. There is also the possibility that some patients with EH in our study were admitted to the department of endocrinology and metabolism because their baseline plasma aldosterone was relatively higher than average, and these participants were excluded from the PA group via a confirmatory test. Since the difference between the plasma aldosterone levels in patients with PA and patients with EH was not as significant as that shown by Redheuil et al. [22], the results of the two studies are discordant.

Animal experiments have shown that chronic elevation of aldosterone can cause myocardial fibrosis, which may result from oxidative stress, inflammation, and fibrillar collagen accumulation [31,39-41]. The Eplerenone in Mild Patients Hospitalization And SurvIval Study in Heart Failure (EMPHASIS-HF) trial showed that mineralocorticoid receptor antagonists (MRAs) may have a beneficial effect in the early stages of heart failure [41], implying that excessive exposure to aldosterone may lead to ventricular remodeling in patients with PA. MRAs are also recommended in the 2016 guidelines [2]. We found that patients with PA demonstrated significantly greater ventricular remodeling compared to those with EH. It is important that patients with PA should undergo evaluation for ventricular remodeling using either echocardiography or cardiac MRI immediately after diagnosis. As the emergence of newer techniques, such as compressed sensing, might make cardiac MRI more accessible, it could be used more commonly for the multi-parametric evaluation of ventricular remodeling [42]. Moreover, useful information derived from cardiac MRI could guide early intervention with pharmacotherapy aimed at reversing remodeling in patients demonstrating early-stage ventricular remodeling.

Some limitations of the present study should be noted. First, the sample size of our study was relatively small; thus, future studies with larger sample sizes with patients of different ages and PA subtypes that represent both sexes are needed. Second, this was a single-center cross-sectional study. Further research is needed to confirm and expand these findings. Third, echocardiography is a commonly used cardiac imaging method for evaluating LV structure and function, and the study lacked a comparison between the cardiac MRI and echocardiography results of LV remodeling in patients with PA versus those with EH. A systematic comparison between echocardiography and cardiac MRI is required in future research.

In conclusion, patients with PA exhibited greater ventricular hypertrophy and enlargement, as well as myocardial fibrosis, compared to patients with EH. Cardiac MRI T1 mapping possesses the ability to detect myocardial fibrosis in patients with PA.

Supplement

The Supplement is available with this article at https://doi.org/10.3348/kjr.2020.1291.

Conflicts of Interest

The authors have no potential conflicts of interest to disclose.

Author Contributions

Conceptualization: Jiayu Sun, Yan Ren, Tao Wu. Data curation: Wei Cheng, Shuai He, Lu Tang, Qiao Deng. Formal analysis: Lu Tang, Qiao Deng. Funding acquisition: Jiayu Sun, Yan Ren. Investigation: Xiumin Liu, Lei Li, Wei Wag, Fangli Zhou. Methodology: Tao Wu. Project administration: Jiayu Sun. Resources: Jiayu Sun, Yan Ren. Software: Xiaoyue Zhou. Supervision: Jiayu Sun, Yan Ren. Validation: Tao Wu. Visualization: Tao Wu. Writing—original draft: Tao Wu. Writing—review & editing: Tao Wu, Jiayu Sun, Yan Ren, Yucheng Chen, Wei Wang, Fangli Zhou.

ORCID iDs
Tao Wu
https://orcid.org/0000-0002-0593-5070
Yan Ren
https://orcid.org/0000-0003-4519-397X
Wei Wang
https://orcid.org/0000-0002-7105-3711
Wei Cheng
https://orcid.org/0000-0003-3959-7548
Fangli Zhou
https://orcid.org/0000-0002-5500-5736
Shuai He
https://orcid.org/0000-0001-5048-5999
Xiumin Liu
https://orcid.org/0000-0003-3779-6383
Lei Li
https://orcid.org/0000-0002-6929-8621
Lu Tang
https://orcid.org/0000-0003-0403-7209
Qiao Deng
https://orcid.org/0000-0001-7456-4851
Xiaoyue Zhou
https://orcid.org/0000-0002-7094-4731
Yucheng Chen
https://orcid.org/0000-0002-0601-8039
Jiayu Sun
https://orcid.org/0000-0002-0920-5948

REFERENCES

1. Byrd JB, Turcu AF, Auchus RJ. Primary aldosteronism: practical approach to diagnosis and management. *Circulation* 2018;138:823-835
2. Funder JW, Carey RM, Mantero F, Murad MH, Reincke M, Shibata H, et al. The management of primary aldosteronism: case detection, diagnosis, and treatment: an endocrine society clinical practice guideline. *J Clin Endocrinol Metab* 2016;101:1889-1916
3. Monticone S, D'Ascenzo F, Moretti C, Williams TA, Veglio F, Gaita F, et al. Cardiovascular events and target organ damage in primary aldosteronism compared with essential hypertension: a systematic review and meta-analysis. *Lancet Diabetes Endocrinol* 2018;6:41-50
4. Milliez P, Girerd X, Plouin PF, Blacher J, Safar ME, Mourad JJ. Evidence for an increased rate of cardiovascular events in patients with primary aldosteronism. *J Am Coll Cardiol* 2005;45:1243-1248
5. Udelson JE. Left ventricular shape: the forgotten stepchild of remodeling parameters. *JACC Heart Fail* 2017;5:179-181
6. Kirkpatrick JN, St John Sutton M. Assessment of ventricular remodeling in heart failure clinical trials. *Curr Heart Fail Rep* 2012;9:328-336
7. Tomoaia R, Beyer RS, Simu G, Serban AM, Pop D. Understanding the role of echocardiography in remodeling after acute myocardial infarction and development of heart failure with preserved ejection fraction. *Med Ultrason* 2019;21:69-76
8. Yang Y, Zhu LM, Xu JZ, Tang XF, Gao PJ. Comparison of left ventricular structure and function in primary aldosteronism and essential hypertension by echocardiography. *Hypertens Res* 2017;40:243-250
9. Lee HH, Hung CS, Wu XM, Wu VC, Liu KL, Wang SM, et al. Myocardial ultrasound tissue characterization of patients with primary aldosteronism. *Ultrasound Med Biol* 2013;39:54-61
10. Vasan RS, Evans JC, Benjamin EJ, Levy D, Larson MG, Sundstrom J, et al. Relations of serum aldosterone to cardiac structure: gender-related differences in the Framingham Heart Study. *Hypertension* 2004;43:957-962
11. Basman C, Parmar YJ, Kronzon I. Intracardiac echocardiography for structural heart and electrophysiological interventions. *Curr Cardiol Rep* 2017;19:102
12. Bai AD, Steinberg M, Showler A, Burry L, Bhatia RS, Tomlinson GA, et al. Diagnostic accuracy of transthoracic echocardiography for infective endocarditis findings using transesophageal echocardiography as the reference standard: a meta-analysis. *J Am Soc Echocardiogr* 2017;30:639-646.e8
13. McCrohon JA, Moon JC, Prasad SK, McKenna WJ, Lorenz CH, Coats AJ, et al. Differentiation of heart failure related to dilated cardiomyopathy and coronary artery disease using gadolinium-enhanced cardiovascular magnetic resonance. *Circulation* 2003;108:54-59
14. Choudhury L, Mahrholdt H, Wagner A, Choi KM, Elliott MD, Klocke FJ, et al. Myocardial scarring in asymptomatic or mildly symptomatic patients with hypertrophic cardiomyopathy. *J Am Coll Cardiol* 2002;40:2156-2164
15. Simonetti OP, Kim RJ, Fieno DS, Hillenbrand HB, Wu E, Bundy JM, et al. An improved MR imaging technique for the visualization of myocardial infarction. *Radiology* 2001;218:215-223
16. Reiter U, Reiter C, Kräuter C, Fuchsjäger M, Reiter G. Cardiac magnetic resonance T1 mapping. Part 2: diagnostic potential and applications. *Eur J Radiol* 2018;109:235-247
17. Muscogiuri G, Suranyi P, Schoepf UJ, De Cecco CN, Secinaro A, Wichmann JL, et al. Cardiac magnetic resonance T1-mapping of the myocardium. *J Thorac Imaging* 2018;33:71-80
18. Messroghli DR, Moon JC, Ferreira VM, Grosse-Wortmann L, He T, Kellman P, et al. Clinical recommendations for cardiovascular magnetic resonance mapping of T1, T2, T2* and extracellular volume: a consensus statement by the Society for Cardiovascular Magnetic Resonance (SCMR) endorsed by the European Association for Cardiovascular Imaging (EACVI). *J Cardiovasc Magn Reson* 2017;19:75
19. Salerno M, Kramer CM. Advances in parametric mapping with

https://doi.org/10.3348/kjr.2020.1291

CMR imaging. *JACC Cardiovasc Imaging* 2013;6:806-822
20. van Oorschot JW, Gho JM, van Hout GP, Froeling M, Jansen Of Lorkeers SJ, Hoefer IE, et al. Endogenous contrast MRI of cardiac fibrosis: beyond late gadolinium enhancement. *J Magn Reson Imaging* 2015;41:1181-1189
21. Taylor AJ, Salerno M, Dharmakumar R, Jerosch-Herold M. T1 mapping: basic techniques and clinical applications. *JACC Cardiovasc Imaging* 2016;9:67-81
22. Redheuil A, Blanchard A, Pereira H, Raissouni Z, Lorthioir A, Soulat G, et al. Aldosterone-related myocardial extracellular matrix expansion in hypertension in humans: a proof-of-concept study by cardiac magnetic resonance. *JACC Cardiovasc Imaging* 2020;13:2149-2159
23. Nadruz W. Myocardial remodeling in hypertension. *J Hum Hypertens* 2015;29:1-6
24. Kramer CM, Barkhausen J, Flamm SD, Kim RJ, Nagel E; Society for Cardiovascular Magnetic Resonance Board of Trustees Task Force on Standardized Protocols. Standardized cardiovascular magnetic resonance (CMR) protocols 2013 update. *J Cardiovasc Magn Reson* 2013;15:91
25. de Meester de Ravenstein C, Bouzin C, Lazam S, Boulif J, Amzulescu M, Melchior J, et al. Histological validation of measurement of diffuse interstitial myocardial fibrosis by myocardial extravascular volume fraction from Modified Look-Locker imaging (MOLLI) T1 mapping at 3 T. *J Cardiovasc Magn Reson* 2015;17:48
26. Catena C, Colussi G, Nadalini E, Chiuch A, Baroselli S, Lapenna R, et al. Cardiovascular outcomes in patients with primary aldosteronism after treatment. *Arch Intern Med* 2008;168:80-85
27. Freel EM, Mark PB, Weir RA, McQuarrie EP, Allan K, Dargie HJ, et al. Demonstration of blood pressure-independent noninfarct myocardial fibrosis in primary aldosteronism: a cardiac magnetic resonance imaging study. *Circ Cardiovasc Imaging* 2012;5:740-747
28. Gaddam K, Corros C, Pimenta E, Ahmed M, Denney T, Aban I, et al. Rapid reversal of left ventricular hypertrophy and intracardiac volume overload in patients with resistant hypertension and hyperaldosteronism: a prospective clinical study. *Hypertension* 2010;55:1137-1142
29. Mark PB, Boyle S, Zimmerli LU, McQuarrie EP, Delles C, Freel EM. Alterations in vascular function in primary aldosteronism: a cardiovascular magnetic resonance imaging study. *J Hum Hypertens* 2014;28:92-97
30. Su MY, Wu VC, Yu HY, Lin YH, Kuo CC, Liu KL, et al. Contrast-enhanced MRI index of diffuse myocardial fibrosis is increased in primary aldosteronism. *J Magn Reson Imaging* 2012;35:1349-1355
31. Weber KT, Janicki JS, Pick R, Capasso J, Anversa P. Myocardial fibrosis and pathologic hypertrophy in the rat with renovascular hypertension. *Am J Cardiol* 1990;65:1G-7G
32. Brilla CG, Pick R, Tan LB, Janicki JS, Weber KT. Remodeling of the rat right and left ventricles in experimental hypertension. *Circ Res* 1990;67:1355-1364
33. Okoshi MP, Yan X, Okoshi K, Nakayama M, Schuldt AJ, O'Connell TD, et al. Aldosterone directly stimulates cardiac myocyte hypertrophy. *J Card Fail* 2004;10:511-518
34. Grytaas MA, Sellevåg K, Thordarson HB, Husebye ES, Løvås K, Larsen TH. Cardiac magnetic resonance imaging of myocardial mass and fibrosis in primary aldosteronism. *Endocr Connect* 2018;7:413-424
35. Brooks J, Kramer CM, Salerno M. Markedly increased volume of distribution of gadolinium in cardiac amyloidosis demonstrated by T1 mapping. *J Magn Reson Imaging* 2013;38:1591-1595
36. Puntmann VO, D'Cruz D, Smith Z, Pastor A, Choong P, Voigt T, et al. Native myocardial T1 mapping by cardiovascular magnetic resonance imaging in subclinical cardiomyopathy in patients with systemic lupus erythematosus. *Circ Cardiovasc Imaging* 2013;6:295-301
37. Ntusi NAB, Piechnik SK, Francis JM, Ferreira VM, Matthews PM, Robson MD, et al. Diffuse myocardial fibrosis and inflammation in rheumatoid arthritis: insights from CMR T1 mapping. *JACC Cardiovasc Imaging* 2015;8:526-536
38. Puntmann VO, Voigt T, Chen Z, Mayr M, Karim R, Rhode K, et al. Native T1 mapping in differentiation of normal myocardium from diffuse disease in hypertrophic and dilated cardiomyopathy. *JACC Cardiovasc Imaging* 2013;6:475-484
39. Funder JW. Aldosterone and mineralocorticoid receptors-physiology and pathophysiology. *Int J Mol Sci* 2017;18:1032
40. Sun Y, Zhang J, Lu L, Chen SS, Quinn MT, Weber KT. Aldosterone-induced inflammation in the rat heart: role of oxidative stress. *Am J Pathol* 2002;161:1773-1781
41. Zannad F, McMurray JJ, Krum H, van Veldhuisen DJ, Swedberg K, Shi H, et al. Eplerenone in patients with systolic heart failure and mild symptoms. *N Engl J Med* 2011;364:11-21
42. Nakamura M, Kido T, Kido T, Watanabe K, Schmidt M, Forman C, et al. Non-contrast compressed sensing whole-heart coronary magnetic resonance angiography at 3T: a comparison with conventional imaging. *Eur J Radiol* 2018;104:43-48

 https://doi.org/10.3348/kjr.2020.1291